Evolutionary pathways to NS5A inhibitor resistance in genotype 1 hepatitis C virus

Shuntai Zhou[a,*,1], Sara E. Williford[a,b,1,2], David R. McGivern[a,b], Christina L. Burch[c], Fengyu Hu[a,b,f], Tiffany Benzine[a], Paul Ingravallo[d], Ernest Asante-Appiah[d], Anita Y.M. Howe[d,3], Ronald Swanstrom[a,e], Stanley M. Lemon[a,b,**]

[a] Lineberger Comprehensive Cancer Center, University of North Carolina at Chapel Hill, Chapel Hill, NC, USA
[b] Division of Infectious Diseases, Department of Medicine, University of North Carolina at Chapel Hill, Chapel Hill, NC, USA
[c] Department of Biology, University of North Carolina at Chapel Hill, Chapel Hill, NC, USA
[d] Infectious Diseases, Merck Research Laboratory, Kenilworth, NJ, USA
[e] Department of Biochemistry and Biophysics, University of North Carolina at Chapel Hill, Chapel Hill, NC, USA
[f] Guangzhou Eighth People's Hospital, Guangzhou Medical University, Guangzhou, China

ARTICLE INFO

Keywords:
Primer ID sequencing
Viral evolution
Treatment outcome
Resistance-associated substitution
Reporter virus

ABSTRACT

Direct-acting antivirals (DAAs) targeting NS5A are broadly effective against hepatitis C virus (HCV) infections, but sustained virological response rates are generally lower in patients infected with genotype (gt)-1a than gt-1b viruses. The explanation for this remains uncertain. Here, we adopted a highly accurate, ultra-deep primer ID sequencing approach to intensively study serial changes in the NS5A-coding region of HCV in gt-1a- and gt-1b-infected subjects receiving a short course of monotherapy with the NS5A inhibitor, elbasvir. Low or undetectable levels of viremia precluded on-treatment analysis in gt-1b-infected subjects, but variants with the resistance-associated substitution (RAS) Y93H in NS5A dominated rebounding virus populations following cessation of treatment. These variants persisted until the end of the study, two months later. In contrast, while Y93H emerged in multiple lineages and became dominant in subjects with gt-1a virus, these haplotypes rapidly decreased in frequency off therapy. Substitutions at Q30 and L31 emerged in distinctly independent lineages at later time points, ultimately coming to dominate the virus population off therapy. Consistent with this, cell culture studies with gt-1a and gt-1b reporter viruses and replicons demonstrated that Y93H confers a much greater loss of replicative fitness in gt-1a than gt-1b virus, and that L31M/V both compensates for the loss of fitness associated with Q30R (but not Y93H) and also boosts drug resistance. These observations show how differences in the impact of RASs on drug resistance and replicative fitness influence the evolution of gt-1a and gt-1b viruses during monotherapy with an antiviral targeting NS5A.

1. Introduction

New all-oral, combination direct-acting antiviral (DAA) therapies are highly effective against hepatitis C virus (HCV) and result in sustained virological response (SVR) in most (> 95%) persons with chronic hepatitis C (Bartenschlager et al., 2013). Most DAA combinations used today include an inhibitor of the nonstructural (NS) 5A protein combined with an NS3/4A protease inhibitor and/or an NS5B RNA-dependent RNA polymerase inhibitor. While treatment failure is uncommon, sequencing of HCV RNA after failure typically suggests the presence of drug-resistant viral variants in patients who do not achieve SVR. NS5A inhibitors are a highly potent class of DAA (Gao et al., 2010; Ivanenkov et al., 2017). NS5A is unique to HCV and closely related viruses with multiple essential functions during the viral life cycle, but no known enzymatic activity (Ross-Thriepland and Harris, 2015). NS5A inhibitors have dual modes of action, both impeding viral RNA synthesis by blocking the formation of replicase complexes, and also preventing the intracellular assembly of infectious virions (Benzine et al.,

* Corresponding author.
** Corresponding author. Lineberger Comprehensive Cancer Center, University of North Carolina at Chapel Hill, Chapel Hill, NC, USA.
E-mail addresses: shuntaiz@email.unc.edu (S. Zhou), smlemon@med.unc.edu (S.M. Lemon).
[1] S.Z. and S.E.W. contributed equally to this work.
[2] Current address: S.E.W.: Lahey Hospital & Medical Centre, Burlington, MA.
[3] Current address: A.H.: British Columbia Centre for Excellence in HIV/AIDS, Vancouver, British Columbia, Canada.

https://doi.org/10.1016/j.antiviral.2018.07.024
Received 2 May 2018; Received in revised form 27 July 2018; Accepted 30 July 2018
Available online 03 August 2018

2017; Berger et al., 2014; Boson et al., 2017; McGivern et al., 2014).

HCV is characterized by a high degree of inter- and intra-host diversity, which likely plays an important role in the response to DAAs and development of resistance (Jabara et al., 2014; Smith et al., 2014). There are 7 HCV genotypes that differ by more than 30% at the nucleotide level, with each further divided into subtypes that differ by 20% (Smith et al., 2014). Genotype 1 (gt-1) is the most common globally and in the U.S. Early phase 1 clinical trials of NS5A inhibitors suggested that the antiviral efficacy of NS5A inhibitors was greater in patients with gt-1b versus gt-1a infection (Lawitz et al., 2012; Liu et al., 2015). Amino acid substitutions in NS5A associated with antiviral resistance ('resistance-associated substitutions' or RASs) also differ between gt-1a and gt-1b viruses (Issur and Gotte, 2014; Lontok et al., 2015; Zeuzem et al., 2017). Amino acid substitutions conferring at least a 2.5-fold reduction in susceptibility to an NS5A inhibitor (daclatasvir, ledipasvir, pibrentasvir, or elbasvir) have been identified at residues 24, 28, 30, 31, 32, 38, 58, 92, and 93 within domain I of NS5A (Gottwein et al., 2018; HCV Drug Development Advisory Group, 2012; Zeuzem et al., 2017). However, the diversity of RASs appears to be greater in gt-1a than gt-1b viruses (Zeuzem et al., 2017). More importantly, while pre-existing NS5A RASs may negatively impact the SVR rate in gt-1a patients treated with some NS5A inhibitors, such substitutions have limited impact in gt-1b infections (AASLD-IDSA; Zeuzem et al., 2017).

To better understand the evolutionary pathways leading to NS5A inhibitor resistance in gt-1a and gt-1b infection, we used next generation sequencing (NGS) with tagged cDNA primers ("primer ID sequencing") (Jabara et al., 2011; Zhou et al., 2015) to intensively characterize HCV diversity in small cohorts of gt-1a and gt-1b infected patients receiving a 5 day course of elbasvir monotherapy. Primer ID sequencing overcomes several limitations of conventional NGS by eliminating multiple types of PCR-related errors, thereby allowing unprecedented sequencing depth and accuracy (overall error rate ~0.01%) (Jabara et al., 2011; Zhou et al., 2015). Each template consensus sequence (TCS) generated by primer ID sequencing represents an original viral RNA template queried at the very first cDNA synthesis step, making primer ID sequencing an excellent tool to study highly diversified viral populations such as HIV-1 and HCV (Barnard et al., 2016; Jabara et al., 2014; Keys et al., 2015; Zhou et al., 2016). Coupling this approach with a unique set of serial serum samples collected before, during and after five days of elbasvir monotherapy, we show here that gt-1a and gt-1b HCV acquire antiviral resistance through distinct selection pathways, and that genotype-specific differences in RAS linkage and frequency can be linked to differences in cell culture assays of viral fitness.

2. Materials and methods

2.1. Study participants, clinical samples, and primer ID sequencing

Serial plasma samples were collected from subjects participating in a phase 1b clinical trial in which they received either elbasvir (10 mg or 50 mg q.d.) monotherapy or placebo for 5 days (MK-8742 P002 trial, ClinicalTrials.gov Identifier: NCT01532973) (Liu et al., 2015). Seven subjects were infected with gt-1a HCV (4 receiving 50 mg of elbasvir, 2 10 mg of elbasvir, and 1 placebo) and 6 subjects were infected with gt-1b virus (5 receiving 50 mg elbasvir and 1 placebo). RNA encoding domain I of NS5A (amino acids 23–123) was sequenced in an average of 6 serum samples from each subject, collected between 0 (pre-treatment) and 60 days after the initiation of therapy (Table S1). Primer ID libraries were constructed using previously published protocols and primer sequences shown in Table S2 (Zhou et al., 2015, 2016). Multiplexed libraries were sequenced using Illumina MiSeq (Illumina, San Diego, CA) 300 bp paired-end sequencing.

2.2. Bioinformatics and phylogenetic analysis

The Illumina bcl2fastq pipeline (v 1.8.4) was used for initial demultiplexing of the data and TCS pipeline (v 1.3.2) to create primer ID template consensus sequences (TCSs) (available at https://github.com/SwanstromLab/PID). In-house scripts were generated to derive abundances of substitutions at each nucleotide and amino acid position in each sample. The primer ID approach allowed identified linkages within each TCS, and neighbor-joining trees were built with MUSCLE (v 3.8.31) (Edgar, 2004a; b).

2.3. In vitro replicative fitness assays

The impact of RASs on replicative fitness and drug resistance were determined using recombinant cell culture-adapted gt-1a H77S.3/GLuc2A (Shimakami et al., 2011) and gt-1b N.2/Gluc2A (Yamane et al., 2014) reporter viruses expressing *Gaussia princeps* luciferase (GLuc). RASs were introduced into plasmid DNAs using Quikchange XL site-directed mutagenesis (Agilent). Plasmids were linearized with *Xba*I and transcribed in vitro to produce HCV genomic RNA with the T7 Megascript kit (Ambion, Austin, TX). Huh7 2-3c cells were electroporated with the RNA and replication fitness assessed by monitoring secreted GLuc activity as described previously (Mauger et al., 2015; Shimakami et al., 2011).

3. Results

3.1. Primer ID MiSeq sequencing of HCV RNA in serial plasma samples

Approximately 3000 to 12,000 TCSs were obtained from each clinical sample, providing a sampling depth of 0.1%–0.03% (defined as the abundance of minor variants with a 95% chance of being detected) (Table S1). However, extremely low or undetectable levels of viremia precluded sequencing of virus in samples collected between 1 and 13 days after starting elbasvir therapy in all gt-1b and some gt-1a-infected subjects.

3.2. Pre-therapy resistance-associated substitutions and intra-host diversity

We considered that differences in the genetic diversity of gt-1a and gt-1b viruses could contribute to differences in the development of NS5A inhibitor resistance and thus treatment outcome. We thus examined the frequency of pre-treatment polymorphisms at the most relevant 16 amino acid positions between codons 23 and 123 of NS5A (Fig. 1A). Significant baseline intra- and inter-host variation existed at codons 28, 30 and 93 (positions of several important RASs), but the intra-host average pairwise diversity (π) of the baseline nucleotide sequences of the viral populations did not differ significantly between gt-1a and gt-1b subjects ($\pi = 0.87$ vs. 0.82, $p = 0.30$). We also calculated estimated genetic distances using the model-based Tamura-Nei method (TN93 distance) which assesses the distribution of pairwise distances between sequences (Tamura and Nei, 1993). Three of 7 gt-1a subjects (subjects 1, 2, and 5) but only 1 of 6 gt-1b subjects (subject 12) showed a high frequency of TCSs with a TN93 distance greater than 0.04 substitutions/site ($p = 0.24$ by χ^2 test) (Fig. 1B and C). The existence of multiple peaks in the frequency distributions of TN93 distance suggest that these subjects had several distinct viral lineages before therapy.

3.3. Elbasvir-induced changes in sequence encoding NS5A domain I

We calculated Shannon's entropy as a measure of the variability of amino acid residues at each position within the NS5A protein (Korber et al., 1994). Significant elbasvir-induced changes occurred between baseline and day 28 in gt-1a virus infected subjects at codons 28, 30, 31, 58, and 93 (Fig. S1), and in gt-1b subjects at codons 28, 31, and 93 (Fig. S2). Significant changes in the frequency of amino acid polymorphisms were evident by day 1, but not 4hr after the start of elbasvir therapy. In contrast, no changes were observed in Shannon's entropy at any position in subjects (7 and 13) receiving placebo.

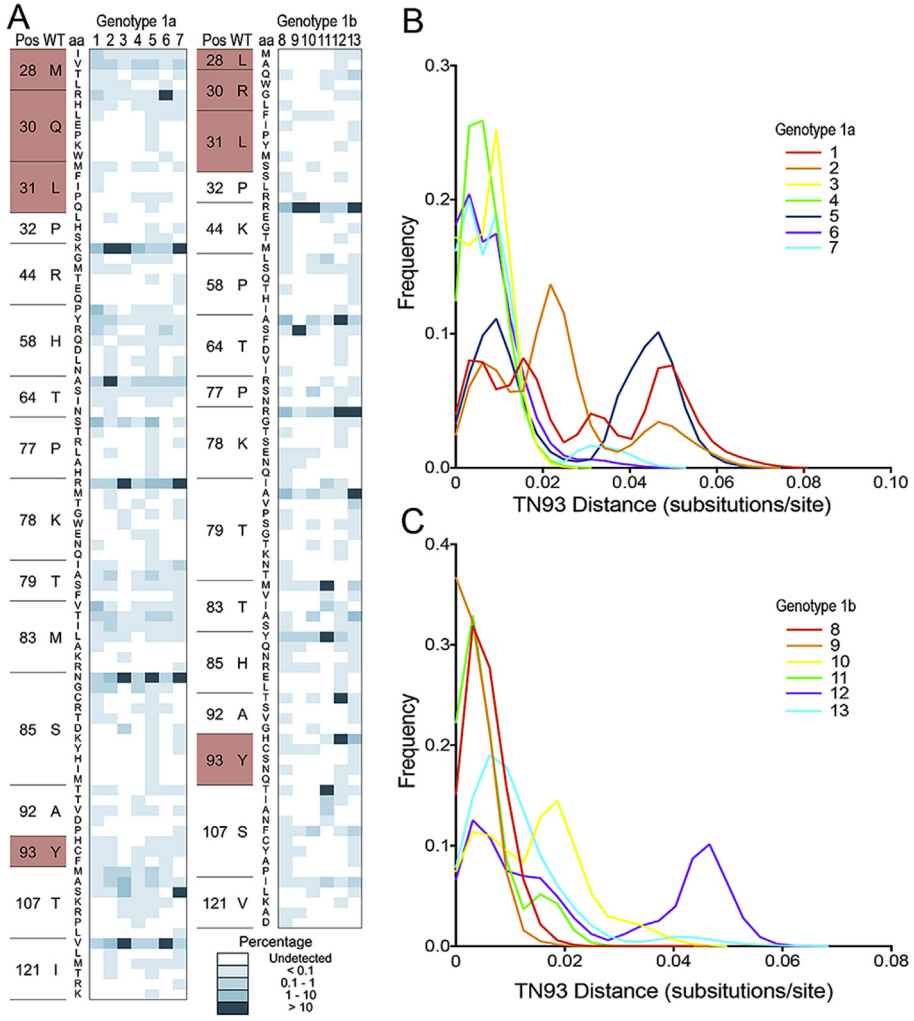

Fig. 1. Pre-treatment intra-host diversity in HCV RNA encoding domain 1 of NS5A. (A) Baseline heat map of amino acid substitutions at potential RAS positions in domain I of NS5A in subjects with gt-1a (subjects 1–7) and gt-1b (subjects 8–13) infections. Positions analyzed include those identified by elbasvir-induced changes in Shannon's entropy (see Figs. S1 and S2). Frequencies of specific substitutions are shown in different colors for each subject at each position (see key at bottom). Highlighted positions are major sites of RASs previously reported. Pos, position; WT, wildtype; aa, amino acid. **(B** and **C)** Distributions of TN93 distances of baseline HCV viral populations in gt-1a (B) and gt-1b (C) subjects. The x-axis is the TN93 distance (substitutions per site), the y-axis shows the frequency of TN93 distance. Multiple peaks on the distribution plot suggests that the viral population is comprised of multiple distinct variants.

3.4. Evolutionary pathways to NS5A inhibitor resistance in gt-1a virus

Since primer ID sequencing retains information concerning linkage between substitutions, subsequent analyses focused on the linkage between changes at codons 28, 30, 31, and 93, determining haplotypes defined by these positions at each timepoint. As an example, Subject 2 was infected with gt-1a HCV and recieved 10 mg elbasvir (Table S1). At baseline the viral population was homogenous at all four codons, with M28, Q30, L31 and Y93 ("MQLY" haplotype, Fig. 2A, top). By day 2, the viral population had changed dramatically, consistent with a substantial, greater than 3.0 $\log_{10}$ drop in the level of viremia (Fig. 2A, bottom). The original consensus MQLY haplotype had declined to only 14% of the population, and haplotypes with Y93H (MQLH) and L31M (MQMY) dominated with frequencies of 41% and 23%, respectively. Minor haplotypes included those with Q30R (MRLY), Q31H (MHLY) Q30E (MELY), or M28T (TRLY), each at ~5%.

These variants evolved throughout the 5-day treatment period and continued to change in frequency after therapy with the emergence of new haplotypes (Fig. 2A). Variants with Y93H were most abundant at day 4 (79% MQLH), but quickly declined in frequency after cessation of therapy (17% by day 12) and were largely absent by day 60. Y93N (MQLN) represented 4% of the population at day 4, increased to 14% at days 9 and 12, and similarly decreased to ~1% by day 60. In contrast, variants with substitutions at position 30 (MRLY, MELY, and MRMY) began to increase in frequency off drug at day 6, becoming dominant as the viremia rebounded to the baseline level. Variants with substitutions at codon 31 (MQMY and MQVY) persisted at a frequency of 5–10% at the end of the study. Thus, we documented two major pathways to drug resistance in this subject: (1) Y93H/N/S/C, and (2) Q30R/E/H with or without L31M, with less common pathways to resistance including L31M/V, and M28T with or without Q30R. Temporal changes in the relative frequencies of individual haplotypes on and off therapy were likely driven by differences in degrees of elbasvir resistance and replicative fitness. Importantly, we never observed Y93H and Q30R in the same lineage.

Both of these major resistance pathways were observed in 5 of the 6 gt-1a subjects (Fig. 2A and Fig. S3). Subject 6, in whom Q30R was dominant at baseline (98% MRLY), was an exception (Fig. 2B). This subject experienced less than a 2 $\log_{10}$ drop in viremia by day 6 despite treatment with 50 mg elbasvir daily. The baseline MRLY haplotype decreased in frequency during and off treatment, dropping to only 6% by the end of the study. L31M/V substitutions began to emerge within the background of Q30R on day 1, with an MRVY haplotype becoming dominant at day 7, and increasing to 92% by day 60 when viremia was greater than 10-fold that at baseline.

3.5. Evolutionary pathways of NS5A inhibitor resistance in gt-1b virus

In gt-1b infected subjects, we observed little or no change in haplotype frequencies 4 h after starting elbasvir, but found viremia suppressed so severely by day 1 that changes in the viral population could not be assessed. Major changes were observed in rebounding virus populations, however. For example, viral rebound was sufficient in subject 8 by day 21 to determine that the baseline consensus LRLY

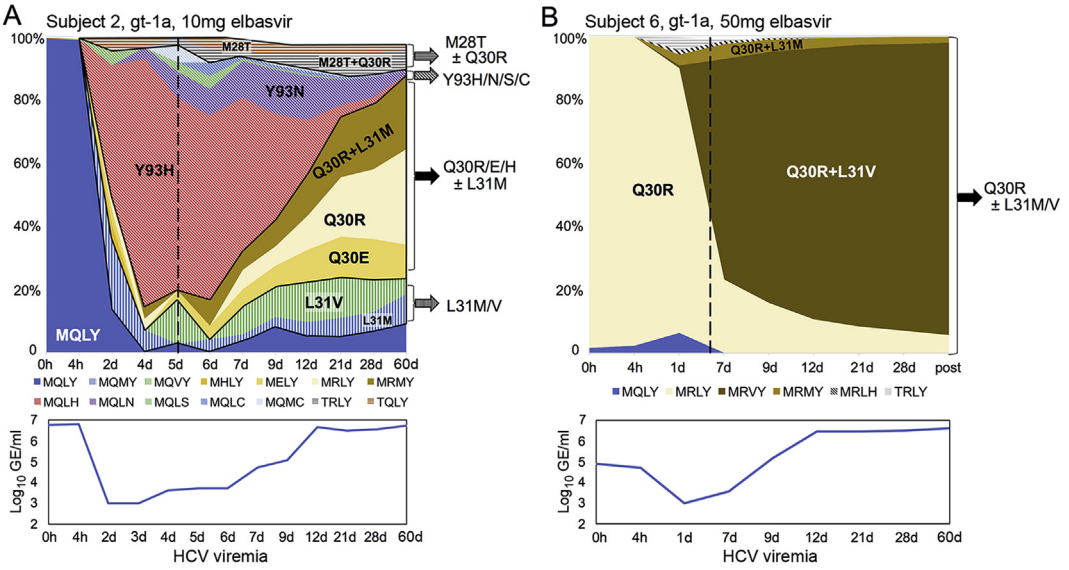

Fig. 2. Evolutionary pathways to elbasvir resistance in gt-1a-infected subjects. (**A**) gt-1a infected subject 2. (**B**) gt-1a-infected subject 6 with a dominant pre-existing Q30R substitution. Haplotypes defined by sequence at amino acid positions 28, 30, 31 and 93 (see text) are shown at the bottom of each graph. Dashed lanes indicate when the elbasvir monotherapy ended.

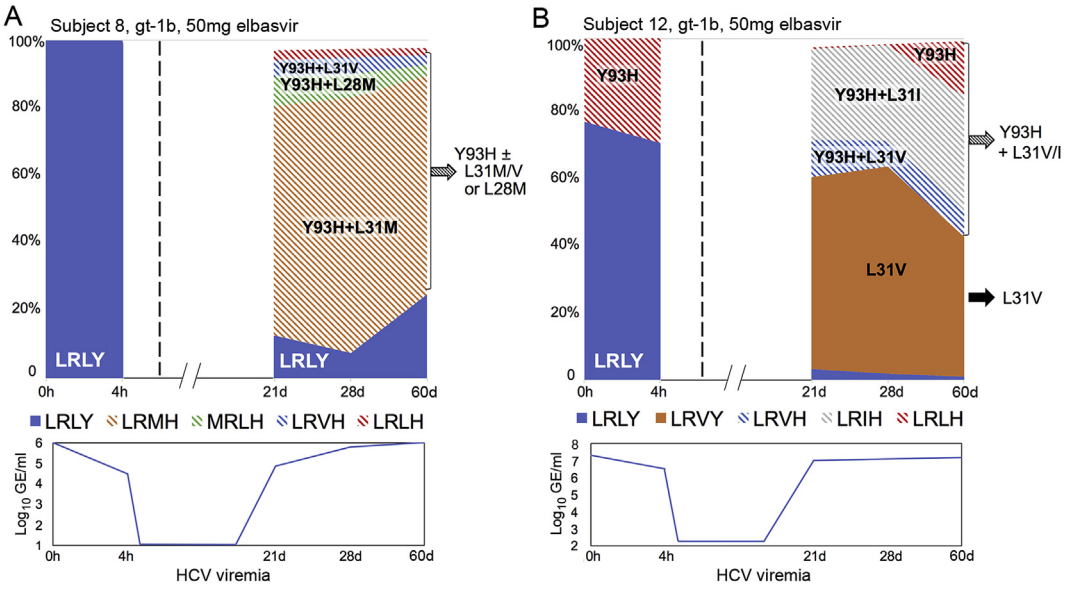

Fig. 3. Evolutionary pathways to elbasvir resistance in gt-1b-infected subjects. (**A**) gt-1b-infected subject 8. (**B**) gt-1b-infected subject 12, with a high-frequency of pre-existing variants with a Y93H substitution. See legend to Fig. 2 for additional details.

haplotype (100%) had been largely replaced by a haplotype with dual Y93H and L31M substitutions (68% LRMH, Fig. 3A). MRLH, LRVH and LRLH haplotypes were also present as minor variants. Unlike what we observed in gt-1a infected subjects, gt-1b haplotypes with Y93H persisted off therapy and remained dominant at the end of the study (Fig. 3A). Resistant variants emerged in a similar fashion in subjects 9, 10 and 11 who were also infected with gt-1b virus (Fig. S3). In each, Y93H was dominant in the rebounding viral population and persisted with or without concomitant L31M/V or L28M substitutions, whereas the baseline consensus haplotype was detectable but remained at a low levels throughout follow-up.

Subject 12, who had a high frequency of Y93H at baseline (24% LRLH), was an exception among the gt-1b subjects (Fig. 3B). The baseline consensus haplotype, LRLY, was decreased in frequency by 4 h, and present at very low frequency when viremia rebounded at 21 days. Variants with an L31V substitution (LRVY) were dominant in the rebounding virus population (Fig. 3B), but over time this haplotype was partially replaced by an increasing frequency of Y93H variants (LRLH, LRVH, and LRIH haplotypes) which persisted to the end of the study.

3.6. Genetic structure of HCV populations before and after elbasvir treatment

We performed phylogenetic analyses to further examine the linkage between RASs and the genetic structure of viral populations. Fig. 4 compares the phylogenetic trees of HCV in subjects with gt-1a and gt-1b infections at baseline and following elbasvir treatment. In the 1a-infected subject shown (subject 4, Fig. 4A), resistant variants with Y93H/N substitutions can be seen to have arisen by day 7 in multiple independent lineages, some very closely related to baseline lineages. Importantly, there were no lineages with both Y93H/N and Q30R substitutions, consistent with the linkage analysis described above.

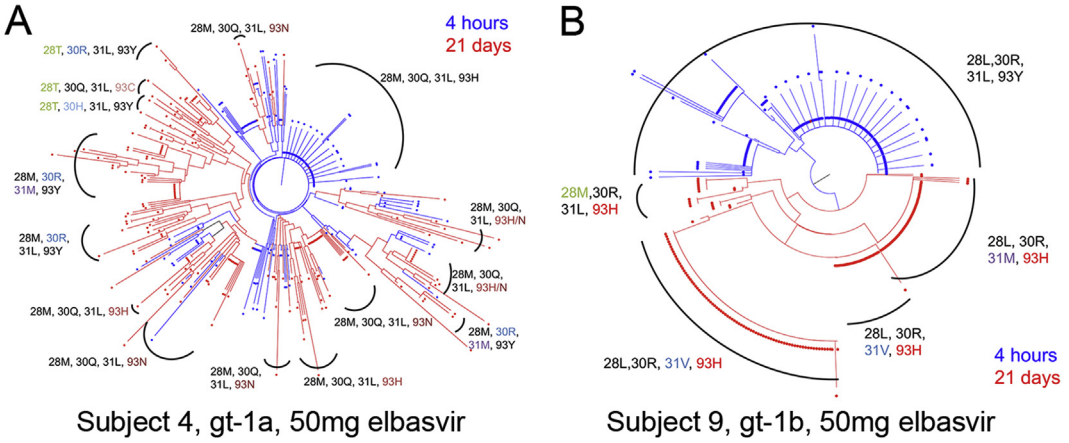

Fig. 4. Phylogenetic trees of sequences obtained at 0 h and first available data point after the 5-day therapy. (**A**) gt-1a-infected subject 4, (**B**) gt-1b-infected subject 9. Sequences in blue were obtained from the 0-h sample whereas those in red are from the 7-day sample and 21-day sample for subjects 4 and 9, respectively. Haplotyes defined by amino acid residues at positions 28, 30, 31 and 93 are labeled with each major viral linage. Residues shown in black font represent baseline (consensus sequence) whereas those in color are RASs.

Similar evolutionary patterns were observed in other gt-1a subjects receiving elbasvir (Fig. S4). In contrast, in gt-1b-infected subjects (for example subject 9, Fig. 4B), the viral population shifted completely post-therapy as Y93H emerged and persisted in novel lineages, some with additional substitutions on top of Y93H, such as L28M, L31V, and L31M. With the exception of subject 12, phylogenetic patterns were similar in the other gt-1b-infected subjects (Fig. S5). In contrast, population structures were stable in placebo recipients (Figs. S6 and S7).

3.7. RAS impact on replicative fitness and drug susceptibility of gt-1a and gt-1b virus

Both drug resistance and replicative fitness influence how viral variants emerge and persist with antiviral therapy. To see whether in vitro measurements of these parameters might explain the differences we observed between gt1-1a and gt-1b-infected subjects, we used luciferase-expressing gt-1a (H77S.3/GLuc2A, MQLY haplotype) and gt-1b (N.2/GLuc2A, LRLY) reporter viruses (Beard et al., 1999; Yamane et al., 2014; Yi et al., 2006) (Fig. 5A). GLuc expression by these viruses provides a measure of their replication. Preliminary studies demonstrated that the EC_{50} of elbasvir (determined 72 h after drug addition) was lower for the gt-1a (2.2 pM) than the gt-1b reporter virus (7.1 pM). The maximal inhibition achieved with concentrations of elbasvir ≥250 pM was also greater for the gt-1a versus gt-1b virus at 48 ($p < 0.0001$ by two-sided *t*-test) and 72 h ($p = 0.0033$) after addition of drug (Fig. 5B). Since NS5A inhibitors impede RNA replication by blocking assembly of the replicase complex, this suggests a significantly shorter half-life for the gt-1a replicase complex (Benzine et al., 2017; McGivern et al., 2014). These findings are consistent with previously published work indicating that elbasvir is at least as potent against gt-1a as gt -1b viruses (Liu et al., 2015).

Although replicon studies indicate Y93H/N substitutions cause the highest levels of elbasvir resistance in both gt-1a and gt-1b HCV, reported fold-increases in EC_{50} were only 17 for gt-1b compared to 220–929 for gt-1a (Liu et al., 2015). The capacity of gt-1a virus to sustain greater elbasvir resistance than gt-1b may thus have contributed to higher levels of viremia during treatment in gt-1a than gt-1b infected subjects. Y93H also caused a much greater loss of replicative fitness in the gt-1a reporter virus: the gt-1a MQLH haplotype replicated at only 3% the level of the wild-type MQLY, whereas the gt-1b LRLH haplotype was 41% as fit as LRLY (Fig. 5C). Replicon studies suggest other gt-1b strains may be more negatively impacted by Y93H substitutions (Liu et al., 2015), but these results are consistent with the persistence of gt-1b and not gt-1a Y93H variants post-treatment (Figs. 2 and 3, and Fig.

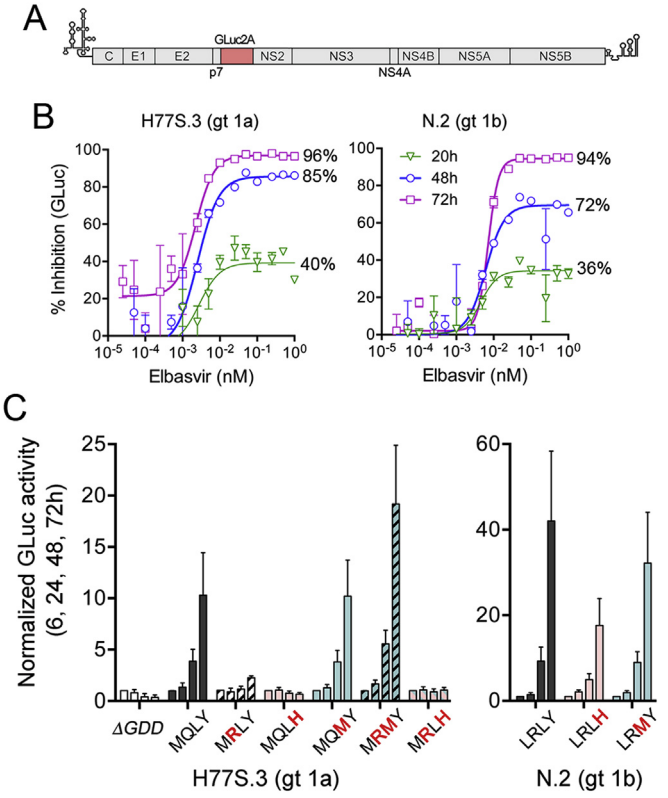

Fig. 5. Impact of RASs on replicative fitness of gt-1a and gt-1b reporter viruses. (**A**) Genome organization of gt-1a H77S.3/GLuc2A and gt-1b N.2/GLuc2A reporter viruses that express *Gaussia princeps* luciferase (GLuc) from sequence inserted upstream of the NS5A-coding region, between p7 and NS2 (Yamane et al., 2014). (**B**) Inhibition of GLuc secretion by cells infected with (*left*) gt-1a H77S.3/GLuc2A or (*right*) N.2/GLuc2A viruses 20, 48 or 72 h after the addition of elbasvir at the indicated concentrations. Results represent the mean ± SEM of 3 technical replicates. (**C**) Huh7 cells were transfected with genomic RNAs representing NS5A haplotypes indicated by the single letter-code for the amino acid residues present at positions 28,30, 31 and 93, with genotype consensus amino acid residues in black and RASs shown in red font. Secreted GLuc activity was measured at 6, 24, 48 and 72hr post transfection, with results normalized to activity at 6h (arbitrarily set to 1.0). Data shown represent the mean ± S.E.M. of 3 independent experiments, each with 3 technical replicates. *ΔGDD* is replication-incompetent H77S RNA carrying a lethal mutation in the active site of the NS5B RNA-dependent RNA polymerase.

S3).

Similar studies help to explain the second-site L31M/V substitutions we observed in gt-1a subjects with Q30R (Fig. 2 and Fig. S5). Q30R causes a 16-fold increase in the EC_{50} of gt-1a replicons (Liu et al., 2015), and this substitution was frequent in the gt-1a subjects we studied (Fig. 2 and Fig. S5). However, as noted above, Q30R and Y93H/N substitutions emerged in distinct lineages, and were never found together in a single lineage. Consistent with this, while Q30R (MRLY haplotype) caused a only 4.6-fold loss of fitness in gt-1a virus, combining it with Y93H (MRLH haplotype) was lethal and resulted in no detectable replication (Fig. 5C). In contrast, combining Q30R with L31M (which by itself had no impact on gt-1a replication fitness) completely reversed the loss of fitness resulting from Q30R (Fig. 5C, MRMY haplotype) and also boosted elbasvir resistance from 16-fold to 1489-fold (Table S3). The combination of Q30R and L31V was even more resistant (7143-fold, Table S3). These results explain why Q30R and Y93H were never found in the same lineage, and why Q30R emergence was typically associated with second-site L31M substitutions in gt-1a subjects.

4. Discussion

While NS5A inhibitors are an important component of effective DAA combination therapies for both gt-1a and gt-1b HCV infection, treatment outcome is generally superior in gt-1b-infected persons (Lawitz et al., 2012; Liu et al., 2015). This cannot be attributed to differences in drug potency, as reflected in EC_{50} values, and the reasons for this difference remain uncertain. We show here that gt-1a and gt-1b viruses differ fundamentally in the way in which resistant variants emerge and persist off therapy, and that some of these differences correlate with genotype-specific differences in the impact of RASs on resistance and replicative fitness.

Our study is unique among others that have examined the response of HCV to NS5A inhibitors. The use of primer ID sequencing eliminated errors commonly introduced by PCR as well as sequencing platform artifacts existing in conventional next generation sequencing strategies (Jabara et al., 2011; Keys et al., 2015; Lee et al., 2017; Zhou et al., 2015). It also allowed us to identify linkage between RASs. The method was sufficiently sensitive to accurately detect minority variants with frequencies as low as 0.03%–0.1% in the viral population (a function of the number of viral genomes actually sequenced). The number of subjects we studied was relatively small, and of necessity limited by the intensity of the analysis. However, the changes we observed in HCV populations during and after elbasvir therapy are likely representative of those occurring generally in gt-1a and gt-1b infected patients, and provide new insight into how resistance to NS5A inhibitors evolves.

In gt-1a infected subjects, we observed two major independent pathways to resistance (Fig. 6). Y93H/C/N substitutions emerged during treatment, but rapidly diminished in frequency off therapy, becoming minor variants 2 months later. Q30R and L31M/V substitutions were also observed early in treatment, but these RASs, either individually or in combination, increased in frequency following cessation of therapy. The dominance of Y93H during treatment may be explained by its far greater resistance to elbasvir (220-fold increase in EC_{50}) compared to Q30R (16-fold) (Liu et al., 2015) (Table S3). On the other hand, the much greater replicative fitness of Q30R versus Y93H (Fig. 5C) explains the expansion of Q30R genomes off treatment (Fig. 6). Moreover, in vitro data show that second-site L31M substitutions fully rescue the fitness of virus with Q30R (Fig. 5C), contributing to Q30R persistence and dramatically boosting elbasvir resistance (Table S3). Interestingly, while we detected Q30R at baseline in all 7 gt-1a infected subjects (Fig. 1A), it was dominant in only one (subject 6, Fig. 2B). A review of the Los Alamos database found Q30R present in only 13 of 3018 (0.4%) gt-1a sequences.

In contrast to gt-1a infected subjects, we observed only a single pathway to resistance in those with gt-1b infection (Fig. 6). Viremia was

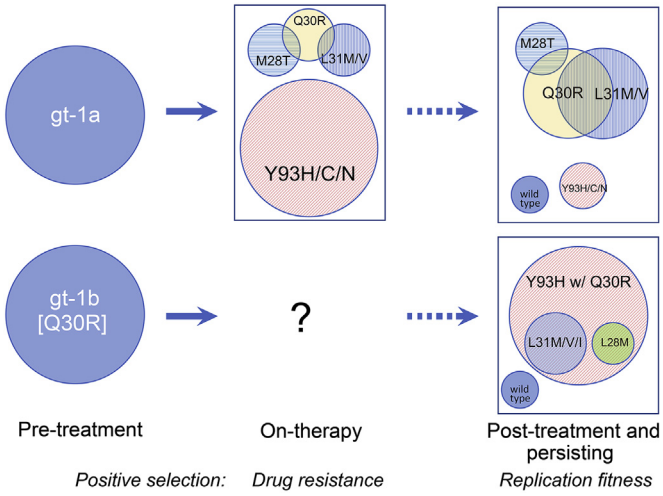

Fig. 6. Major evolutionary pathways to NS5A resistance in subjects infected with gt-1a and gt-1b HCV infection. Changes in the NS5A domain I sequence of gt-1a and gt-1b virus are shown in overlapping or independent Venn diagrams during and after treatment with elbasvir according to the single letter amino acid code for residues at positions 28, 30, 31, and 93. The size of each circle is roughly proportionate to their frequencies in the viral population. The emergence and persistence of variants is driven by positive selective forces related to the magnitude of drug resistance during therapy, and relative replicative fitness subsequently. Note that gt-1a virus has two distinct pathways to resistance, while only one was observed in gt-1b infections.

extremely low during elbasvir treatment of these subjects. The effective size of the replicating viral population is thus likely to have been much smaller in the gt-1b than gt-1a subjects during therapy, most likely because even the most resistant Y93H and L31F gt-1b variants demonstrate only 15- to 17-fold increases in EC_{50} (Liu et al., 2015). In contrast to gt-1b infected subjects, where rebounding resistant virus populations demonstrated fundamentally altered structures, RASs emerged from multiple preexisting viral linages in gt-1a subjects (Fig. 4A and Fig. S6). This suggests that the effective population size on therapy was sufficiently large in these patients to allow for the deterministic selection of RASs. All possible RASs are likely to have been present before the treatment due to the error-prone nature of HCV RNA synthesis, emerging with drug selection pressure when replication is not fully suppressed. In gt-1b, the limited effective population size during therapy may have allowed only the most resistant variants (Y93H pathway) to be selected.

Unfortunately, available crystallographic models of NS5A structure provide little insight into why the evolution of inhibitor resistance differs in gt-1a and gt-1b viruses. There are several domain I structures reported, but none include the amino-terminal 35 amino acids, and thus we do not know how 3 critical residues (positions 28, 30 and 31) are positioned within the molecule. Moreover, models of the gt-1a (Lambert et al., 2014) and gt-1b (Tellinghuisen et al., 2005) structures differ in that gt-1b is a dimer, while gt-1a is a tetramer, with the relative positioning of the monomer subunits different in each. It is not clear which of these models reflects the native conformation of NS5A, and it is possible that the molecule adopts both folds. A complete molecular explanation for the findings we describe here must thus await a better understanding of the NS5A structure and its association with other components of the HCV replication complex.

Declaration of interest

SML has received royalties from AbbVie and grant funding from Merck and Gilead Sciences. DRM has received grant funding from AbbVie and Gilead Sciences. RS is a co-inventor on patents related to primer ID sequencing and has received nominal royalties. EA-A and P.I.

are employees of Merck, Sharp and Dohme. All other authors have no competing interests.

Acknowledgements

We thank Drs. Christoph Welsch and Joseph Marcotrigiano for stimulating discussions. This work was funded by a research grant from the Investigator-Initiated Studies Program of Merck, Sharp and Dohme (SML) and grants from the National Institutes of Health [T32-AI007151 (SEW), R01-AI095690 (SML), R21-AI115207 (DRM), R56-AI44667 (RS). This work also received infrastructure support from the UNC Center for AIDS Research [NIH award P30 AI50410] and the UNC Lineberger Comprehensive Cancer Center [NIH award P30 CA16068]. The funders had no role in study design, data collection and analysis, decision to publish, or preparation of the manuscript.

Appendix A. Supplementary data

Supplementary data related to this article can be found at https://doi.org/10.1016/j.antiviral.2018.07.024.

References

AASLD-IDSA Recommendations for Testing, Managing, and Treating Hepatitis C. http://www.hcvguidelines.org.

Barnard, R., Chopra, A., James, I., Blinco, J., Watson, M.W., Jabara, C.B., Hazuda, D., Lemon, S.M., Mallal, S., Gaudieri, S., 2016. Primer ID ultra-deep sequencing reveals dynamics of drug resistance-associated variants in breakthrough hepatitis C viruses: relevance to treatment outcome and resistance screening. Antivir. Ther. 21, 567–577.

Bartenschlager, R., Lohmann, V., Penin, F., 2013. The molecular and structural basis of advanced antiviral therapy for hepatitis C virus infection. Nat. Rev. Microbiol. 11, 482–496.

Beard, M.R., Abell, G., Honda, M., Carroll, A., Gartland, M., Clarke, B., Suzuki, K., Lanford, R., Sangar, D.V., Lemon, S.M., 1999. An infectious molecular clone of a Japanese genotype 1b hepatitis C virus. Hepatology 30, 316–324.

Benzine, T., Brandt, R., Lovell, W.C., Yamane, D., Neddermann, P., De Francesco, R., Lemon, S.M., Perelson, A.S., Ke, R., McGivern, D.R., 2017. NS5A inhibitors unmask differences in functional replicase complex half-life between different hepatitis C virus strains. PLoS Pathog. 13, e1006343.

Berger, C., Romero-Brey, I., Radujkovic, D., Terreux, R., Zayas, M., Paul, D., Harak, C., Hoppe, S., Gao, M., Penin, F., Lohmann, V., Bartenschlager, R., 2014. Daclatasvir-like inhibitors of NS5A block early biogenesis of hepatitis C virus-induced membranous replication factories, independent of RNA replication. Gastroenterology 147, 1094–1105 e1025.

Boson, B., Denolly, S., Turlure, F., Chamot, C., Dreux, M., Cosset, F.L., 2017. Daclatasvir prevents hepatitis C virus infectivity by blocking transfer of the viral genome to assembly sites. Gastroenterology 152, 895–907 e814.

Edgar, R.C., 2004a. MUSCLE: a multiple sequence alignment method with reduced time and space complexity. BMC Bioinf. 5, 113.

Edgar, R.C., 2004b. MUSCLE: multiple sequence alignment with high accuracy and high throughput. Nucleic Acids Res. 32, 1792–1797.

Gao, M., Nettles, R.E., Belema, M., Snyder, L.B., Nguyen, V.N., Fridell, R.A., Serrano-Wu, M.H., Langley, D.R., Sun, J.H., O'Boyle 2nd, D.R., Lemm, J.A., Wang, C., Knipe, J.O., Chien, C., Colonno, R.J., Grasela, D.M., Meanwell, N.A., Hamann, L.G., 2010. Chemical genetics strategy identifies an HCV NS5A inhibitor with a potent clinical effect. Nature 465, 96–100.

Gottwein, J.M., Pham, L.V., Mikkelsen, L.S., Ghanem, L., Ramirez, S., Scheel, T.K.H., Carlsen, T.H.R., Bukh, J., 2018. Efficacy of NS5A inhibitors against hepatitis C virus genotypes 1-7 and escape variants. Gastroenterology 154, 1435–1448.

HCV Drug Development Advisory Group, 2012. Clinically relevant HCV drug resistance mutations. Ann. Forum Collab HIV Res. 14, 1–10.

Issur, M., Gotte, M., 2014. Resistance patterns associated with HCV NS5A inhibitors provide limited insight into drug binding. Viruses 6, 4227–4241.

Ivanenkov, Y.A., Aladinskiy, V.A., Bushkov, N.A., Ayginin, A.A., Majouga, A.G., Ivachtchenko, A.V., 2017. Small-molecule inhibitors of hepatitis C virus (HCV) non-structural protein 5A (NS5A): a patent review (2010-2015). Expert Opin. Ther. Pat. 27, 401–414.

Jabara, C.B., Hu, F., Mollan, K.R., Williford, S.E., Menezes, P., Yang, Y., Eron, J.J., Fried, M.W., Hudgens, M.G., Jones, C.D., Swanstrom, R., Lemon, S.M., 2014. Hepatitis C Virus (HCV) NS3 sequence diversity and antiviral resistance-associated variant frequency in HCV/HIV coinfection. Antimicrob. Agents Chemother. 58, 6079–6092.

Jabara, C.B., Jones, C.D., Roach, J., Anderson, J.A., Swanstrom, R., 2011. Accurate sampling and deep sequencing of the HIV-1 protease gene using a Primer ID. Proc. Natl. Acad. Sci. U. S. A. 108, 20166–20171.

Keys, J.R., Zhou, S., Anderson, J.A., Eron Jr., J.J., Rackoff, L.A., Jabara, C., Swanstrom, R., 2015. Primer ID informs next-generation sequencing platforms and reveals pre-existing drug resistance mutations in the HIV-1 reverse transcriptase coding domain. AIDS Res. Hum. Retrovir. 31, 658–668.

Korber, B.T., Kunstman, K.J., Patterson, B.K., Furtado, M., McEvilly, M.M., Levy, R., Wolinsky, S.M., 1994. Genetic differences between blood- and brain-derived viral sequences from human immunodeficiency virus type 1-infected patients: evidence of conserved elements in the V3 region of the envelope protein of brain-derived sequences. J. Virol. 68, 7467–7481.

Lambert, S.M., Langley, D.R., Garnett, J.A., Angell, R., Hedgethorne, K., Meanwell, N.A., Matthews, S.J., 2014. The crystal structure of NS5A domain 1 from genotype 1a reveals new clues to the mechanism of action for dimeric HCV inhibitors. Protein Sci. 23, 723–734.

Lawitz, E.J., Gruener, D., Hill, J.M., Marbury, T., Moorehead, L., Mathias, A., Cheng, G., Link, J.O., Wong, K.A., Mo, H., McHutchison, J.G., Brainard, D.M., 2012. A phase 1, randomized, placebo-controlled, 3-day, dose-ranging study of GS-5885, an NS5A inhibitor, in patients with genotype 1 hepatitis C. J. Hepatol. 57, 24–31.

Lee, S.K., Zhou, S., Baldoni, P.L., Spielvogel, E., Archin, N.M., Hudgens, M.G., Margolis, D.M., Swanstrom, R., 2017. Quantification of the latent HIV-1 reservoir using ultra deep sequencing and primer ID in a viral outgrowth assay. J. Acquir. Immune Defic. Syndr. 74, 221–228.

Liu, R., Curry, S., McMonagle, P., Yeh, W.W., Ludmerer, S.W., Jumes, P.A., Marshall, W.L., Kong, S., Ingravallo, P., Black, S., Pak, I., DiNubile, M.J., Howe, A.Y., 2015. Susceptibilities of genotype 1a, 1b, and 3 hepatitis C virus variants to the NS5A inhibitor elbasvir. Antimicrob. Agents Chemother. 59, 6922–6929.

Lontok, E., Harrington, P., Howe, A., Kieffer, T., Lennerstrand, J., Lenz, O., McPhee, F., Mo, H., Parkin, N., Pilot-Matias, T., Miller, V., 2015. Hepatitis C virus drug resistance-associated substitutions: state of the art summary. Hepatology 62, 1623–1632.

Mauger, D.M., Golden, M., Yamane, D., Williford, S., Lemon, S.M., Martin, D.P., Weeks, K.M., 2015. Functionally conserved architecture of hepatitis C virus RNA genomes. Proc. Natl. Acad. Sci. U. S. A. 112, 3692–3697.

McGivern, D.R., Masaki, T., Williford, S., Ingravallo, P., Feng, Z., Lahser, F., Asante-Appiah, E., Neddermann, P., De Francesco, R., Howe, A.Y., Lemon, S.M., 2014. Kinetic analyses reveal potent and early blockade of hepatitis C virus assembly by NS5A inhibitors. Gastroenterology 147, 453–462.

Ross-Thriepland, D., Harris, M., 2015. Hepatitis C virus NS5A: enigmatic but still promiscuous 10 years on!. J. Gen. Virol. 96, 727–738.

Shimakami, T., Welsch, C., Yamane, D., McGivern, D.R., Yi, M., Zeuzem, S., Lemon, S.M., 2011. Protease inhibitor-resistant hepatitis C virus mutants with reduced fitness from impaired production of infectious virus. Gastroenterology 140, 667–675.

Smith, D.B., Bukh, J., Kuiken, C., Muerhoff, A.S., Rice, C.M., Stapleton, J.T., Simmonds, P., 2014. Expanded classification of hepatitis C virus into 7 genotypes and 67 subtypes: updated criteria and genotype assignment web resource. Hepatology 59, 318–327.

Tamura, K., Nei, M., 1993. Estimation of the number of nucleotide substitutions in the control region of mitochondrial DNA in humans and chimpanzees. Mol. Biol. Evol. 10, 512–526.

Tellinghuisen, T.L., Marcotrigiano, J., Rice, C.M., 2005. Structure of the zinc-binding domain of an essential component of the hepatitis C virus replicase. Nature 435, 374–379.

Yamane, D., McGivern, D.R., Wauthier, E., Yi, M., Madden, V.J., Welsch, C., Antes, I., Wen, Y., Chugh, P.E., McGee, C.E., Widman, D.G., Misumi, I., Bandyopadhyay, S., Kim, S., Shimakami, T., Oikawa, T., Whitmire, J.K., Heise, M.T., Dittmer, D.P., Kao, C.C., Pitson, S.M., Merrill Jr., A.H., Reid, L.M., Lemon, S.M., 2014. Regulation of the hepatitis C virus RNA replicase by endogenous lipid peroxidation. Nat. Med. 20, 927–935.

Yi, M., Villanueva, R.A., Thomas, D.L., Wakita, T., Lemon, S.M., 2006. Production of infectious genotype 1a hepatitis C virus (Hutchinson strain) in cultured human hepatoma cells. Proc. Natl. Acad. Sci. U. S. A 103, 2310–2315.

Zeuzem, S., Mizokami, M., Pianko, S., Mangia, A., Han, K.H., Martin, R., Svarovskaia, E., Dvory-Sobol, H., Doehle, B., Hedskog, C., Yun, C., Brainard, D.M., Knox, S., McHutchison, J.G., Miller, M.D., Mo, H., Chuang, W.L., Jacobson, I., Dore, G.J., Sulkowski, M., 2017. NS5A resistance-associated substitutions in patients with genotype 1 hepatitis C virus: prevalence and effect on treatment outcome. J. Hepatol. 66, 910–918.

Zhou, S., Bednar, M.M., Sturdevant, C.B., Hauser, B.M., Swanstrom, R., 2016. Deep sequencing of the HIV-1 env gene reveals discrete X4 lineages and linkage disequilibrium between X4 and R5 viruses in the V1/V2 and V3 variable regions. J. Virol. 90, 7142–7158.

Zhou, S., Jones, C., Mieczkowski, P., Swanstrom, R., 2015. Primer ID validates template sampling depth and greatly reduces the error rate of next-generation sequencing of HIV-1 genomic RNA populations. J. Virol. 89, 8540–8555.